JOURNAL OF CATALYSIS 119, 121–134 (1989)

Formation of Crystalline Compounds and Catalyst Deactivation during SO_2 Oxidation in V_2O_5–$M_2S_2O_7$ (M = Na, K, Cs) Melts

S. BOGHOSIAN,* R. FEHRMANN,† N. J. BJERRUM,† AND G. N. PAPATHEODOROU*

*Institute of Chemical Engineering and High Temperature Chemical Processes, University of Patras, GR-26110 Patras, Greece, and †Chemistry Department A, Technical University of Denmark, DK-2800 Lyngby, Denmark

Received September 22, 1988; revised January 18, 1989

The formation of low-valence crystalline vanadium compounds was studied in the V_2O_5–$M_2S_2O_7$ (M = Na, K, Cs) unsupported melt systems in the temperature range 350–480°C during SO_2 oxidation with unconverted 10% SO_2, 11% O_2, and 79% N_2 as the feed gas. A gas–molten-salt reactor system was built to provide the possibility of isolating the crystalline precipitates under operating conditions at any temperature by filtering the catalyst melts. Both V(IV) and V(III) crystalline compounds were formed under different process conditions. The V(IV) compounds $K_4(VO)_3(SO_4)_5$, $Na_2VO(SO_4)_2$, and $Cs_2(VO)_2(SO_4)_3$ and the V(III) compounds $KV(SO_4)_2$, $NaV(SO_4)_2$, and $CsV(SO_4)_2$ were isolated from the melts. A drop in the catalytic activity was observed at temperatures where these compounds started to precipitate. For the first time it has been possible to observe the drop in catalytic activity and the formation of low-soluble vanadium compounds *simultaneously*. It was also found that (i) high alkali-to-vandium ratios, large alkali cation promoters, or mixing of the alkali promoters caused the precipitation and the steep activity drop to occur at lower temperatures, and (ii) the crystalline precipitates of V(IV) and V(III) could be redissolved by a heat treatment at/or above 470°C or by purging the melts with N_2. The thermal stability of the V(IV) compounds has been investigated by means of DTA. Furthermore the decomposition rate of $KV(SO_4)_2$ and $K_4(VO)_3(SO_4)_5$ during isothermal heating at different temperatures in the range 470–510°C has been measured and IR spectra of the decomposition products have been recorded and interpreted. The results indicate that a heat treatment of melts containing large amounts of V(IV) and V(III) precipitates leads to reoxidation of vanadium to the +V oxidation state. Certain conditions required for reactivation of deactivated catalysts are pointed out and are discussed in relation to the dissolution of the precipitates in the melts.

INTRODUCTION

The oxidation of sulfur dioxide, catalyzed by the alkali-promoted vanadium catalysts, has been the subject of numerous investigations during the last four decades due to the importance of this reaction for the industrial production of sulfuric acid. It is now well established that under operating conditions the catalyst is a molten salt consisting of V_2O_5 dissolved in alkali pyrosulfates. The oxidation of SO_2 takes place as a homogeneous reaction in the liquid phase, which is dispersed on an inert support (*1–3*). Despite persistent research efforts, fundamental technical problems concerning the sulfuric acid catalyst remain unresolved with a major problem being the sudden drop of activity at temperatures below 440°C (*1*). Due to this factor, the minimum temperature at which available catalysts are able to operate is almost 50°C higher than the temperature that would lead to a conversion higher than 99.8% for a once-through process. Thus, in order to achieve high conversions, sulfuric-acid plants use converters with an intermediate absorption of SO_3 before the last catalyst bed.

Arrhenius plots of the apparent rate constant for the SO_2 oxidation on commercial catalysts as well as on catalysts supported on CPG (Controlled Pore Glass) invariably show a break at temperatures typically below 450°C while the apparent activation en-

0021-9517/89 $3.00

ergy is often very high in the low-temperature region (*4–8*). This phenomenon seems to be connected to the presence of vanadium species of lower oxidation state at low temperatures. As indicated by high-temperature ESR measurements (*9*), there are two different V(IV) species in the catalyst. The ESR signal of one of these species starts to grow at temperatures below 480°C, and is assigned to a crystalline compound that accumulates at the expense of the solute V(IV) complexes. This precipitation leads to an elimination of the active vanadium species and seems to be the reason for the progressive deactivation of the catalyst at temperatures below 440°C. The sharp break in the Arrhenius plots has been attributed to the precipitation of V(IV) (*1, 5, 7, 8, 10*). The break disappeared by taking the precipitation into account in the kinetic model (*5, 7*). Nevertheless, there has so far been no report on the isolation—and characterization—of any V(IV) precipitate from the catalyst under operation conditions.

Detailed investigations of exchanging potassium with sodium (*11, 12*) or cesium (*8, 10, 12, 13*) revealed that (i) generally, the promoting effect increases with increasing alkali atomic number, (ii) the addition of some sodium to the potassium-promoted catalyst has a beneficial effect on the low-temperature activity, and (iii) the cesium-promoted catalyst undergoes deactivation at temperatures below 400°C.

It is believed (*1, 2*) that the reasons for the strange low-temperature behavior of the catalyst are to be found not only in transport resistances, or kinetic and mechanistic alterations, but also in the chemistry of the molten V_2O_5–$K_2S_2O_7$ system which has been investigated recently (*14–18*). The molten system in contact with SO_2, SO_3, O_2, and N_2 gas mixtures represents a very realistic model of the potassium-promoted catalyst. Therefore, the isolation and characterization of compounds that precipitate in this system are considered important. It should be noted here that a previous article dealing with a V(IV) solid compound formed in the molten V_2O_5–$K_2S_2O_7$ system under catalyst operation conditions (*19*) described the isolation of compounds after the melts were cooled to room temperature. The aim of the present study was to investigate simultaneously the catalytic activity and the formation of low-valence vanadium compounds in the unsupported V_2O_5–$M_2S_2O_7$ (M = Na, K, Cs) melts during SO_2 oxidation. The experiments and the reactor system were designed in a way that ensured the isolation of the precipitating compounds *under operating conditions.*

EXPERIMENTAL

Apparatus

The gas–molten salt reactor was built in such a way as to facilitate the isolation of crystalline precipitates under experimental conditions similar to those of industrial catalytic systems. The very fast heat transfer through the homogeneous liquid phase of the (continuously stirred) unsupported melts led to negligible temperature gradients. During activity measurements, the reactor was operated differentially in order to minimize concentration gradients in the bulk phase.

The flow diagram of the gas–molten salt reactor is shown in Fig. 1. (A more detailed description of the apparatus can be found elsewhere (*20*).) The gas mixing unit had five Brooks (Model 5850) mass flow controllers with flow ranges as shown in Fig. 1. The gases used were SO_2 (Matheson, 99.98% anhydrous), N_2 (Linde, 99.999%), and O_2 (Linde, 99.99%). The nitrogen and oxygen streams were passed through molecular sieves and activated charcoal traps before entering the mass flow controllers. One of the three SO_2 streams (Fig. 1) was led directly to a mixing point before the reactor, whereas the gas mixture produced by the rest of the flow controllers could be fed to a preconverter. The preconverter exit gas was mixed with the SO_2 bypassing stream and thus any desired amount of preconversion could be achieved before the

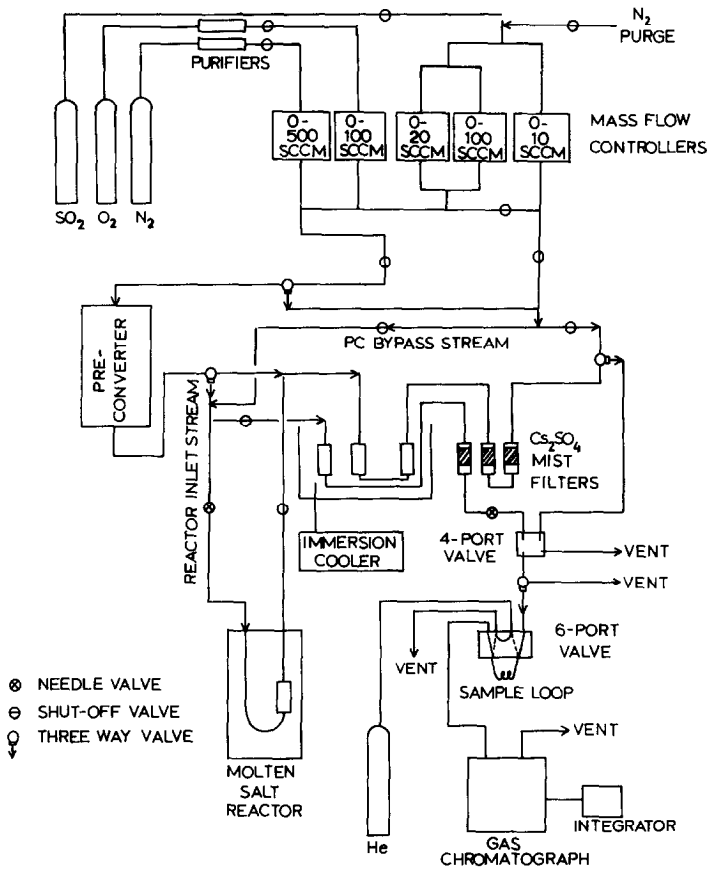

FIG. 1. Gas–molten-salt reactor flow diagram.

gas was fed to the molten salt reactor. By means of three-way valves the preconverter feed gas, the preconverter exit gas, and the molten-salt reactor inlet gas could be analyzed and the preconversion could be determined.

The preconverter was made of borosilicate 5-cm-o.d. glass tubing equipped with stainless-steel fittings on top and bottom and was vertically mounted inside the cylindrical core of an aluminum block furnace that could be operated up to 500°C. The catalyst was platinated silica produced by reduction of silica wetted by a solution of H_2PtCl_6 with formaldehyde (40% technical grade) and was placed on a sintered glass frit. The preconverter was operated at 395°C giving 99% conversion of the feed gas with a flow rate up to 70 cm^3/min.

The gas stream withdrawn for analysis at the molten-salt reactor inlet was sent through stainless-steel and Viton tubing to an SO_3 cold trap made of borosilicate glass and located inside an antifreeze bath. The temperature of the bath was kept at −35°C by an immersion cooler.

The reactor cell (shown in Fig. 2) was mounted in a holder which was located in an upright position inside a tiltable double-quartz walled tube furnace, in which the temperature was controlled by a proportional controller to within ±2 K. Temperature was measured by a chromel–alumel thermocouple, which was also mounted in the cell holder with the measuring point in contact with the cell area containing the melt. The gas flow was passed through the inlet joint of the reactor cell and sent down-

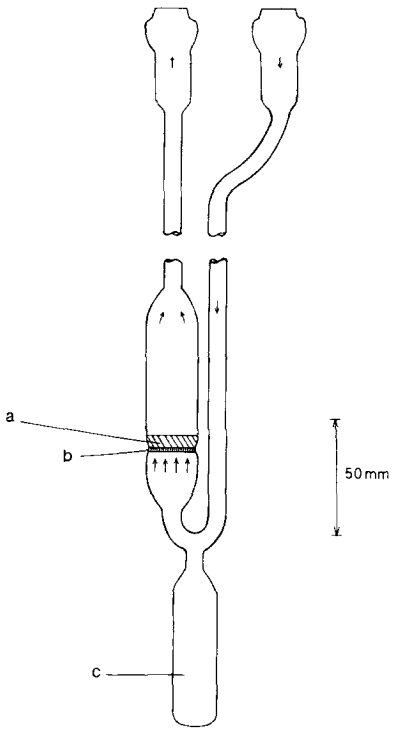

FIG. 2. Molten-salt reactor cell. (a) Catalyst melt, (b) sintered glass-filter disk, (c) bottom ampule for filtrate collection. Arrows indicate direction of flow during catalyst operation. The flow direction is reversed for filtering the melts and isolating the crystalline precipitates.

ward along a tube where it was heated to the reactor temperature before bubbling through the catalyst melt (a), which was located above a sintered glass-filter disk with a diameter of 1–2 cm (b). Visual inspection of the melt during operation was possible through a window in the insulation material of the tube furnace. Mixing was achieved by bubbling the gas through the melt. The reactor setup allowed us to observe the formation of precipitates and enabled us to isolate the solids *under operating conditions*. This isolation could be achieved by switching the reactor inlet gas so it entered through the outlet joint and pressed the melt through the sintered glass-filter disk (b) down into the bottom ampule (c), thus leaving the crystals on the frit.

The reactor exit gas was sent through two SO_3 cold traps (Fig. 1) before flowing toward the gas chromatograph. This was a Perkin–Elmer Sigma 300 with hot-wire detector and two 0.32-cm o.d. and 2.4-m-long stainless-steel columns packed with Porapak Q (80–100 mesh). The gas chromatograph was equipped with a Valco 6-Port external gas sampling valve possessing a 2-ml loop. Before entering the sample loop, the gas streams were passed through Cs_2SO_4 filters for elimination of residual SO_3 gas and sulfuric-acid mist. The chromatograph was operated with He (Linde, 99.999%) as the carrier gas with the columns and the detector operating at 100 and 85°C, respectively. Finally, the chromatographic peak areas were integrated by a Perkin–Elmer LCI-100 computing integrator.

Catalytic activity of the molten-salt catalysts at each temperature was determined as the steady-state turnover frequency, i.e., as (mole SO_2 converted/mole V) s^{-1}. The amount of melt (0.25–0.4 g) and the volumetric flow rate were chosen so that the space velocity was in the range 11,200–23,700 h^{-1}. In this way the conversion was sufficiently low (<15%) to consider the reactor as differential.

Chemicals

The potassium and sodium pyrosulfates were synthesized by thermal decomposition of $K_2S_2O_8$ (Merck, pro analysi) and $Na_2S_2O_8$ (Fluka, pro analysi) and stored in sealed ampules until used as described earlier (*15*). The $Cs_2S_2O_7$ was synthesized by thermal decomposition of $Cs_2S_2O_8$, which was made by anodic oxidation of a $CsHSO_4$ solution using a platinum anode. Details of the procedure will be reported elsewhere (*21(b)*). The purity of the product was checked by measuring the weight loss due to the decomposition reaction $Cs_2S_2O_8 \rightarrow Cs_2S_2O_7 + \frac{1}{2}O_2$ performed under dry N_2 at 300°C. Also a Raman spectrum at 470°C (*21(b)*) of the molten $Cs_2S_2O_7$ shows that the contamination by Cs_2SO_4 and $CsHSO_4$ is below the limit of detection, i.e., below 1%. The nonhygroscopic V_2O_5 (Cerac-

Pure, 99.9%) was used without further purification. All handling of chemicals, including the filling of the reactor cell, was performed in a nitrogen filled glovebox with a water vapor content of ca.1 ppm achieved by continuous recirculation of the box gas through external gas purifiers.

The commercial catalyst investigated was a VK 38 from Haldor Topsøe A/S, Denmark with a content of V_2O_5 on kieselguhr of around 6 wt% and an alkali-to-vanadium ratio of around 3.8 (0.8 Na/V + 3.0 K/V). This catalyst in the form of pellets was crushed gently to a powder before use.

Thermal Analysis

DTA studies of the crystalline compounds that were isolated from the melts were performed on a Dupont Instruments Series 99 Thermal Analyzer. Around 5 mg of each compound was encapsuled in aluminum pans and tested under inert atmosphere (N_2). Measurements of the isothermal decomposition of the compounds contained in platinum cups were performed with the thermal analyzer in the isothermal mode. The heating was interrupted at certain time intervals in order to weigh the cups and estimate the mass loss. The masses were measured with an accuracy of ±0.1 mg.

Infrared Spectra

The infrared spectra were obtained on finely ground powders in pressed KBr disks and recorded on a Perkin–Elmer 297 double beam spectrometer.

RESULTS AND DISCUSSION

Formation of Crystalline Compounds in the V_2O_5–$M_2S_2O_7$ (M = Na, K, Cs) Melts

Molten vanadium pentoxide–alkali pyrosulfate mixtures with alkali-to-vanadium mole ratios ranging between 3 and 10 have been investigated with respect to the precipitation of low-valence vanadium compounds under conditions of low conversions. The composition of the feed gas was 10% SO_2, 11% O_2, 79% N_2, similar to the gas entering the first stage of industrial reactors. For the various promoted melts, the temperature was gradually reduced from the starting temperature, and at each temperature the catalytic melts were allowed sufficient time (up to 24 h) to attain steady state before the conversion was measured.

Below a certain temperature, which depends on the process parameters, the low-soluble V(IV) and V(III) compounds could be observed as small crystals of blue or green, color, respectively. The compounds were isolated from the melts *under operating conditions* described above and were found by means of chemical analysis, X-ray, and spectroscopic methods to have the formulae listed in Table 1.

A characteristic feature for melts with mole ratios $M/V < 5$ is that the blue (V(IV)) compounds dominate the precipitate, whereas increasing amounts of the green (V(III)) compounds are obtained at higher M/V ratios. Compound identification was made by comparing the crystals in a microscope with samples previously analyzed by X-ray and spectroscopic means.

TABLE 1

Crystalline V(IV) and V(III) Salts Formed in the V_2O_5–$M_2S_2O_7$ (M = Na, K, Cs) Melts during SO_2 Oxidation

Alkali promoter	Blue salts (V(IV))	Green salts (V(III))
Na	$Na_2VO(SO_4)_2$[a]	$NaV(SO_4)_2$[b]
K	$K_4(VO)_3(SO_4)_5$[c]	$KV(SO_4)_2$[c]
Cs	$Cs_2(VO)_2(SO_4)_3$[a]	$CsV(SO_4)_2$[b]

[a] Stoichiometry determined by X-ray and chemical analysis. Details will be reported in a later publication (*21b*).

[b] Stoichiometry determined by X-ray analysis.

[c] X-ray structure and spectroscopic properties of $K_4(VO)_3(SO_4)_5$ and $KV(SO_4)_2$ are reported in Refs. (*21a*) and (*22*), respectively.

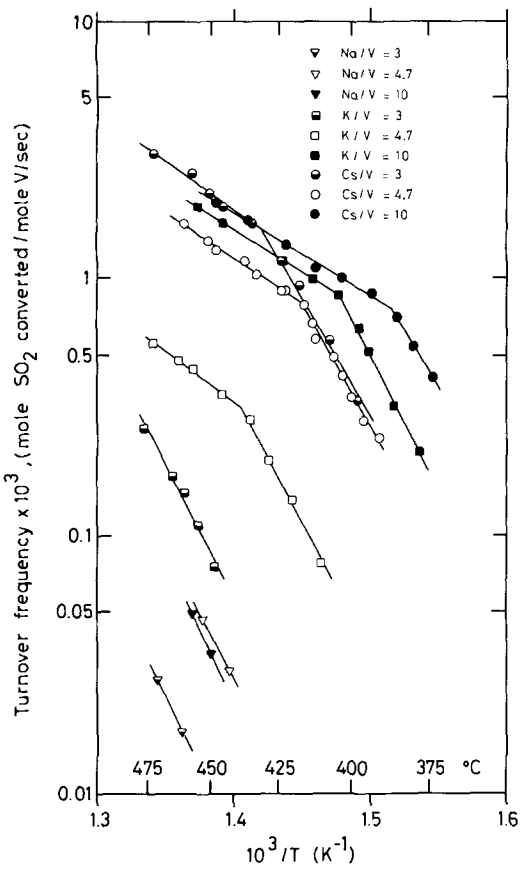

FIG. 3. Arrhenius plots of measured reaction rates for Na-, K-, and Cs-promoted catalyst melts. Feed gas: 10% SO_2, 11% O_2, and 79% N_2. Triangles, squares, and circles refer to Na-, K-, and Cs-promoted melts, respectively. The mole ratio of alkali to vanadium is indicated.

Activity Drop during Compound Precipitation

The activities of the molten-salt catalysts were measured in the temperature range 350–480°C in order to investigate the effect of compound formation on the catalytic activity. Figure 3 shows representative results of such measurements obtained from Na-, K-, and Cs-promoted melts with M/V ratios of 3, 4.7, and 10. Melts with different mixtures of the three promoters at a constant alkali-to-vanadium ratio of 4.7 were also investigated. These results together with the results of the investigation of the commercial catalyst are presented in Figs. 4 and 5. The ratio $M/V = 4.7$ was selected because it represents the eutectic composition of the V_2O_5–$K_2S_2O_7$ binary mixture (*16*) (liquidus temperature: 315°C), while melts with the ratio $M/V = 3$ and 10 were investigated to find the effect of dilution. Arrhenius plots for the investigated melts show, as expected (*4–8*), sharp breaks at temperatures T_b, which are listed in Table 2. The T_b values were reproducible and independent of melt amount and volumetric flow rate within the limits of differential operation of the molten-salt reactor. At temperatures slightly below T_b, formation of crystalline compounds was observed through the window of the furnace.

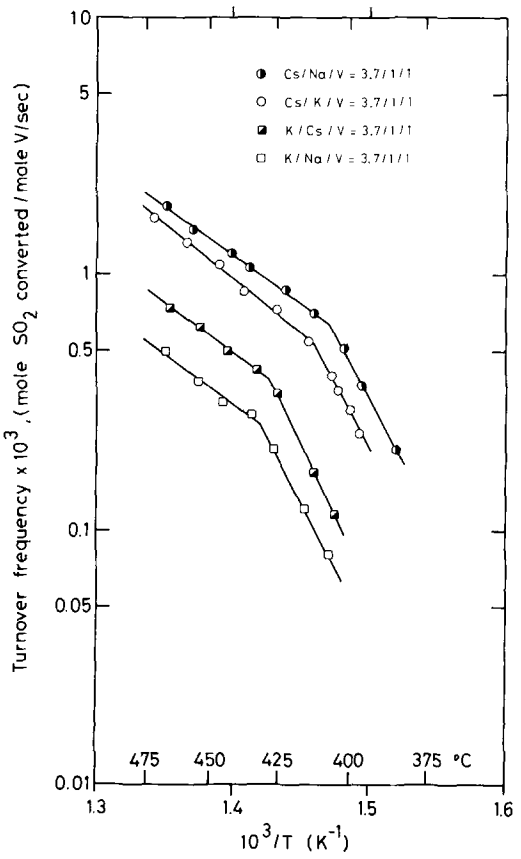

FIG. 4. Arrhenius plots of measured reaction rates for melts containing mixed promoters. Feed gas: 10% SO_2, 11% O_2 and 79% N_2. The mole ratio of alkali to vanadium is indicated.

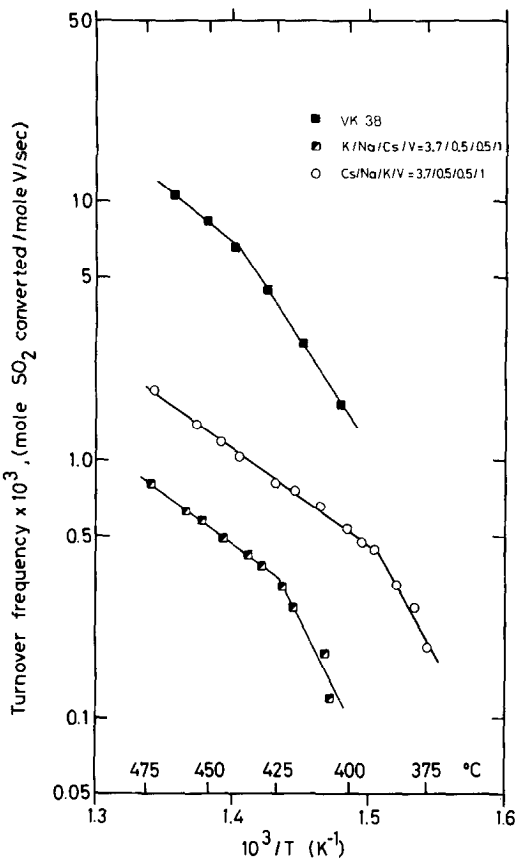

FIG. 5. Arrhenius plots of measured reaction rates for melts containing mixed promoters. Feed gas: 10% SO_2, 11% O_2, and 79% N_2. The mole ratio of alkali to vanadium is indicated.

Table 2 lists the predominating compounds formed in each system studied. However, after each experiment crystals of the green V(III) compounds were also found, in amounts that increased relative to the blue V(IV) compounds with increasing M/V of the melt investigated. Obviously, at T_b the V(IV) and/or the V(III) concentrations are exceeding the solubility limit and the compounds begin to precipitate.

Although the isolation of vanadium precipitates from the working catalyst has never been reported, numerous investigations in the past (*1, 5, 7–10, 13*) have indicated that the sharp activity drop of the K/V catalysts is due to precipitation of a V(IV) complex. Our results for unsupported V_2O_5–$M_2S_2O_7$ melts show that precipitation during SO_2 oxidation indeed occurs in all the systems studied. Furthermore, the isolation of the crystalline blue V(IV) and green V(III) compounds (see Table 1) at temperatures slightly below T_b clearly indicates that the break in the Arrhenius plots (Figs. 3–5) is due to the precipitation of the compounds listed in Table 1. The isolation of the green V(III) compounds indicates that three different oxidation states of vanadium may be involved in the complex chemistry of this catalytic system. The fact that V(III) is difficult to detect by ESR and the signal is found at a high magnetic field, far from the field where V(IV) resonates, might be the reason why precipitation of V(III) complexes has not been reported before.

In the case of the melts where M/V = 3, the results show that the phase transformation starts above 470°C for the Na- and K-promoted melts, whereas it starts at 430°C for the Cs-promoted melt. For the melts where M/V = 4.7, the activity drop occurs at 439, 416, and >460°C for the K-, Cs-, and Na-promoted melts, respectively. Finally, for the melts with M/V = 10 the break points occur at 404, 388, and >460°C, respectively. Thus, increasing atomic number of the alkali metal and increasing mole ratio of the alkali metal to vanadium (M/V) shifts the break point toward a lower temperature. This tendency is in accordance with recent observations (*8*) for melts with molar ratios Cs/V = 2.5, 3, and 3.5, and K/V = 3.5. The specific activity of a promoter tends to increase with the M/V ratio. However, this might be due to a decrease in the mass transport resistance caused by the lower viscosity of the melts with high M/V ratios rather than to an increase in the intrinsic rate. Recent experiments (*23*) free of mass transport resistance show that the specific activity indeed increases when the K/V ratio is decreased from 50 to 4. It should be noted that a large amount of precipitate is observed even at the highest measured temperatures in the case of Na-

TABLE 2

Temperature of the Activity Drop and Compound Formation in the Catalyst Melts[a]

Catalyst melt	T_b, °C[b]	Predominating compounds formed at $T \leq T_b$	Apparent activation energy (kcal/mol)	
			$T > T_b$	$T < T_b$
Na/V = 3	(>470)[c]	$Na_2VO(SO_4)_2$	—	49.2
Na/V = 4.7	(>460)[c]	$Na_2VO(SO_4)_2$	—	49.2
Na/V = 10	(>460)[c]	$Na_2VO(SO_4)_2$, $NaV(SO_4)_2$	—	55.0
K/V = 3	(>475)[c]	$K_4(VO)_3(SO_4)_5$	—	47.0
K/V = 4.7	439	$K_4(VO)_3(SO_4)_5$	17.6	49.2
K/V = 10	404	$K_4(VO)_3(SO_4)_5$, $KV(SO_4)_2$	15.4	47.6
Cs/V = 3	430	$Cs_2(VO)_2(SO_4)_3$	17.8	41.4
Cs/V = 4.7	416	$Cs_2(VO)_2(SO_4)_3$	16.0	42.1
Cs/V = 10	388	$Cs_2(VO)_2(SO_4)_3$, $CsV(SO_4)_2$	14.6	40.9
K/Na/V = 3.7/1/1	432	Blue precipitate	18.1	46.3
K/Cs/V = 3.7/1/1	427	Blue and green precipitate	18.1	50.4
K/Na/Cs/V = 3.7/0.5/0.5/1	424	Blue and green precipitate	17.8	48.2
Cs/K/V = 3.7/1/1	412	Blue and green precipitate	19.3	45.2
Cs/Na/V = 3.7/1/1	407	Blue and green precipitate	17.2	45.4
Cs/Na/K/V = 3.7/0.5/0.5/1	390	Blue and green precipitate	17.2	43.4
VK38 (Haldor Topsøe)	441	The color changes from orange-brown to yellowish-green	18.6	35.6

[a] Feed gas composition: 10% SO_2, 11% O_2, and 79% N_2.

[b] T_b is the temperature at which the compound precipitation and the break in the Arrhenius plots occur simultaneously.

[c] T_b is above the highest measured temperature given in parentheses.

promoted melts. Thus Na alone is a very poor promoter.

It should be emphasized that the data in Figs. 3–5 show the relative activity and not the specific activity and thus cannot be used for comparing the maximum obtainable activities, because the availability of the active vanadium components with our setup is not fully determined by the amount of V_2O_5 in the melt (*1, 7*). On the other hand the data show that the sharp drop of relative activity when the molten salt undergoes phase transformation (precipitation) can be used to compare the values of T_b for the various molten-salt catalytic systems. Thus, an evaluation of a promoter with respect to its influence on the low-temperature activity can be made. This possibility was an important reason for constructing the equipment. The results on the relative activities and temperatures of precipitation for melts with mixed promoters are given in Figs. 4 and 5 and in Table 2. It is evident that substitution of 20% K with Na in a melt where K/V = 4.7, giving a melt where K/Na/V = 3.7/1/1, lowers the T_b from 439 to 432°C. The addition of this amount of Na compares well with the composition of the commercial catalysts, where an enhanced activity in the low-temperature region is also achieved. Substitution with Cs to give a melt where K/Cs/V = 3.7/1/1 leads to an even lower T_b value, i.e., 427°C. Thus Cs seems to be a better additive than Na with respect to an improvement in low-temperature catalytic activity of K-promoted melts. However, mixing all three alkali promoters to give a melt where K/Na/Cs/V = 3.7/0.5/0.5/1 seems to lower the value of T_b a few degrees further, i.e., to 424°C. With respect

to the Cs-promoted melt with Cs/V = 4.7 the T_b value of 416°C is lowered to 412°C by substitution with K to give a melt where Cs/K/V = 3.7/1/1. A further decrease in T_b to 407°C is observed for the melt where Cs/Na/V = 3.7/1/1. Thus Na seems to be a better additive than K for the improvement of the low-temperature activity of Cs-promoted catalysts. An even lower T_b value of 390°C is found for the melt where Cs/Na/K/V = 3.7/0.5/0.5/1. Blue and green precipitates were observed for $T \leq T_b$ in the different melts with mixed promoters, and compounds were isolated. However, the identification of the compounds is rather difficult since a mixture of the low-valence compounds might be obtained and also because salts with mixed cations may form.

Preliminary measurements show that treating the melts with 90% preconverted 10% SO_2, 11% O_2, 79% N_2 feed gas causes the steep activity drop to occur at lower temperatures and indicates the formation of blue (V(IV)) and brown (presumably V(V)) crystalline compounds (*24*).

Our results can be interpreted by considering the following complex equilibria (Eqs. (1)–(4)) in the melts, where the identity of the species put forward is based on previous work (*15–18*) and work in progress (*25*). The first step represents the fixation of SO_2 to a dimeric V(V) complex:

$$(VO_2SO_4)_2S_2O_7^{4-} + SO_2 \rightleftharpoons (VO_2SO_4)_2SO_2^{2-} + S_2O_7^{2-}. \quad (1)$$

The second reaction accounts for the reduction of V(V) to V(IV):

$$(VO_2SO_4)_2SO_2^{2-} \rightleftharpoons (VOSO_4)_2SO_4^{2-}. \quad (2)$$

The third reaction shows the fixation of SO_2 to the dimeric V(IV) complex:

$$(VOSO_4)_2SO_4^{2-} + SO_2 \rightleftharpoons (VOSO_4)_2SO_4SO_2^{2-}. \quad (3)$$

Finally the V(IV) complex undergoes reduction to a V(III) complex:

$$(VOSO_4)_2SO_4SO_2^{2-} \rightleftharpoons 2V(SO_4)_2^{-}. \quad (4)$$

Equations (1)–(4) may express essential steps in the reaction mechanism for the oxidation of SO_2 as well as for the catalyst deactivation. Depending on the type of promoter (Na, K, Cs) the solid compounds listed in Table 1 can be formed from the V(IV) and V(III) complexes of Eqs. (2) and (4). Increased activity of $S_2O_7^{2-}$ in the melt shifts the equilibria ((1)–(4)) involving the three oxidation states toward the formation of V(V) complexes and thus, as has been observed, the temperature of precipitation decreases on going from melts with the composition $M/V = 3$ to melts with the composition $M/V = 10$. It has been shown (*11, 26, 27*) that the ability of the sulfates to take up SO_3 and the stability of pyrosulfates increase in the series Li, Na, K, Rb, Cs, which is probably due to the decreasing polarizing power of the cation in the given series. Work in progress (*25*) shows that indeed the equilibrium between V(IV) and V(V) complexes is shifted more toward the formation of V(V) in molten $Cs_2S_2O_7$ than in $K_2S_2O_7$ indicating a higher activity of $S_2O_7^{2-}$ in the former melt and explains the tendency of the temperature of precipitation to be lower in the order Na, K to Cs in alkali-promoted melts. However, an increased solubility of the low-valence salts with different metal cations in the above series may also account for the difference in T_b. If the solubility is comparable for the Na-, K-, and Cs-low-valence salts then mixing of the promoters should also result in a higher solubility. This may explain the observed shift of T_b toward lower temperatures for the mixed promoter systems as shown in Figs. 4 and 5 and Table 2 and could also account for the increased low-temperature activity of commercial catalysts, where up to 20% of K is substituted by Na. It is well known (*28*) that further substitution with Na leads to a decrease in the catalytic activity.

Our results concerning the relative location of the breaks in the Arrhenius type plots are in agreement with results obtained

for industrial catalysts (*29*) and for catalysts supported on CPG (*8*). However, the values of T_b reported in this work are expected to be higher than the T_b values of SLP catalysts with the same melt composition since the degree of vanadium reduction is considerably higher in unsupported melts and therefore precipitation occurs at somewhat higher temperatures. Results for the commercial catalyst VK 38, which has a composition K/Na/V = 3/0.8/1, show (Fig. 5, Table 2) that the break point appears at 441°C, which is—as expected—somewhat higher (9 K) than that found for the melt where K/Na/V = 3.7/1/1. The apparently high activity of the commercial catalyst is probably due to the support which leads to a better distribution of the active components, thus increasing their availability. A color change of the commercial catalyst from orange-brown to yellowish-green during temperature decrease has also been observed, indicating the formation of lower valence vanadium compounds, but obviously compound isolation was not possible.

The apparent activation energies obtained for the various catalysts are given in Table 2. In the temperature region above T_b this energy is in the range 15–19 kcal/mol (1 cal = 4.184 J), compared to the 16–24 kcal/mol range reported for supported melts (*4, 7, 8, 29, 30*). In the temperature region where precipitation occurs, the apparent activation energy is in the range 41–55 kcal/mol, which compares well with the 50 kcal/mol found for supported melts (*7, 8*). The activation energies of 18.6 and 35.6 kcal/mol found for the commercial catalyst VK 38, in the high- and low-temperature regions, respectively, are the same as those found previously (*29*) for a crushed commercial catalyst of comparable composition.

Thermal Stability of the Compounds and Activity Restoration

The catalytic activity of the molten salts after cooling stepwise in the reactor cell from 480 to 350°C could be restored by heating at temperatures above T_b. During the heat treatment the crystalline V(IV) and V(III) compounds were dissolved into the melt. The DTA curves for the blue V(IV) compounds $K_4(VO)_3(SO_4)_5$, $Na_2VO(SO_4)_2$, and $Cs_2(VO)_2(SO_4)_3$ (Fig. 6) show that at 480°C under inert atmosphere the compounds start to decompose and reoxidize probably by internal oxidation. However, studies of the isothermal decomposition indicated that these compounds can be decomposed at lower temperatures by prolonged heating under inert or oxidizing (i.e., SO_3 or air) atmosphere, as shown in Fig. 7 for $K_4(VO)_3(SO_4)_5$. The green V(III) compounds $KV(SO_4)_2$, $NaV(SO_4)_2$, and $CsV(SO_4)_2$ show a very high thermal stability under inert atmosphere at temperatures up to 500°C but they start to decompose and reoxidize at 470°C in an oxidizing atmosphere, as shown in Fig. 8 for $KV(SO_4)_2$. For both compounds, $K_4(VO)_3(SO_4)_5$ and $KV(SO_4)_2$, the rate of decomposition in-

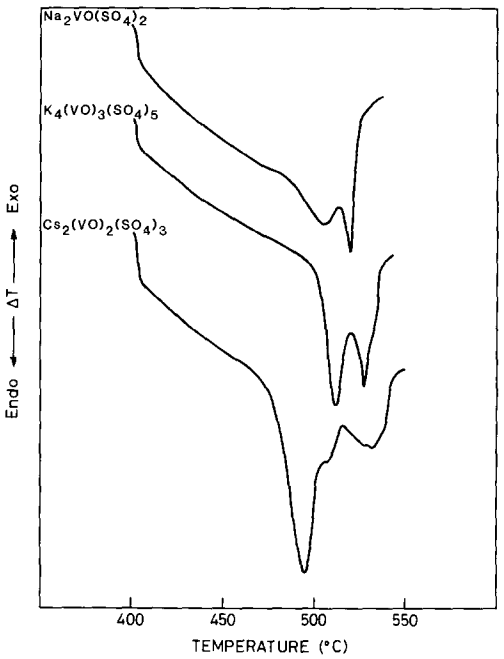

FIG. 6. DTA curves of the compounds $Na_2VO(SO_4)_2$, $K_4(VO)_3(SO_4)_5$, and $Cs_2(VO)_2(SO_4)_3$ measured in inert atmosphere (N_2).

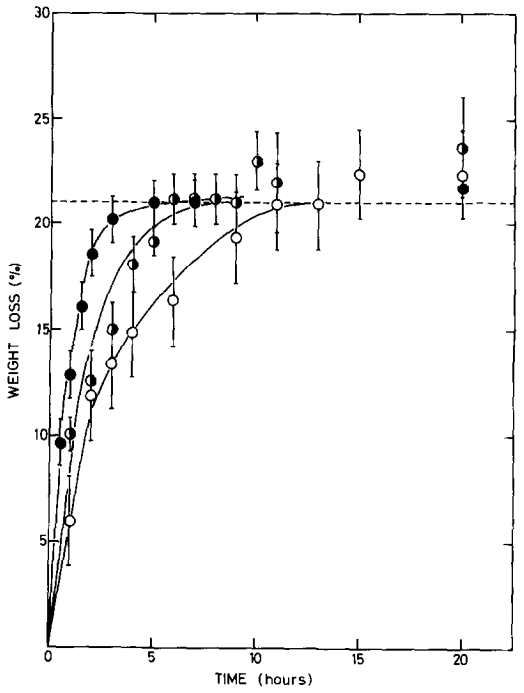

FIG. 7. Plots of weight loss vs time for the compound $K_4(VO)_3(SO_4)_5$ during isothermal heating at 470°C (○), 490°C (◑), and 510°C (●). The dashed line indicates the weight loss corresponding to the possible formation of $4KVO_2SO_4 \cdot K_2SO_4 \cdot 2KVO_3$. The uncertainty of the points reflects the accuracy of the mass measurements of the low mass (5–20 mg) samples.

creased with increasing temperature in the range 470–510°C (Figs. 7 and 8).

A temperature rise lowers the degree of vanadium reduction (9) and consequently shifts the equilibria involving the three oxidation states of vanadium (Eqs. (1)–(4)) toward the formation of V(V) complexes. The crystalline compounds will therefore go into solution for $T > T_b$. Treating the melts with pure N_2 also results in the dissolution of the precipitates. In this case, SO_2 is stripped off and the redox equilibria (i.e., Eq. (1)) will move again toward the formation of V(V) complexes, resulting in dissolution of the crystals. Intensive mixing of the molten salts by bubbling the gas through the melt leads to a fast dissolution of the crystals and to a quick restoration of the catalytic activity contrary to the case of the reactivation of certain deactivated commercial catalysts that exhibits pronounced hysteresis, attributed to slow dissolution of precipitates (*31*). In the latter case complete reversibility leading to a uniform distribution of vanadium in the supported liquid phase is only obtained very slowly by heating the catalyst under air at 460–490°C (*1*) apparently in order to decompose the precipitates.

The IR spectra of the products obtained by heating $K_4(VO)_3(SO_4)_5$ isothermally for different time periods are shown in Fig. 9. In accordance with the observed rate of weight loss for $K_4(VO)_3(SO_4)_5$ the most pronounced change in the IR spectra of the compound takes place within the first 5 h of heating. These changes include a reduction in the number of bands in the region 1000–1300 cm^{-1}, where the ν_3 bands of the SO_4^{2-} group usually are located and weakening of the bands in the region 900–1000 cm^{-1}, where the stretching mode of the VO^{++} unit of V(IV) compounds is found. The features

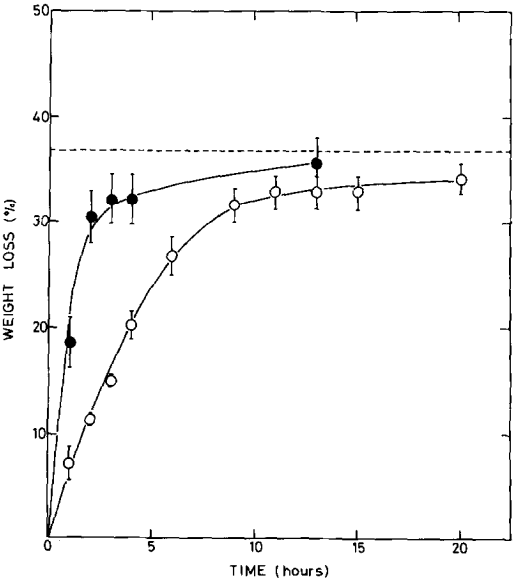

FIG. 8. Plots of weight loss vs time for the compound $KV(SO_4)_2$ during isothermal heating at 470°C (○) and 490°C (●). The dashed line indicates the weight loss corresponding to the possible formation of $KVO_2SO_4 \cdot KVO_3$.

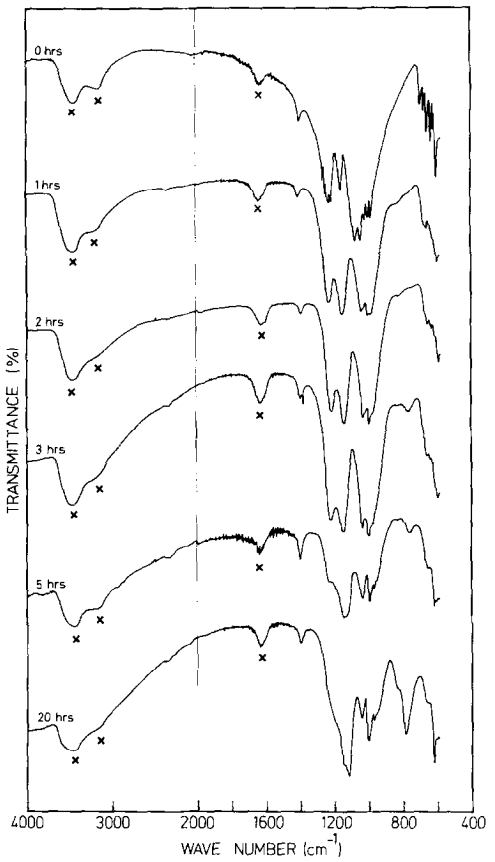

FIG. 9. Infrared spectra of $K_4(VO)_3(SO_4)_5$ after different times of heating in the range 0–20 h at 490°C in nitrogen atmosphere. The spectra were taken from powdered samples pressed in KBr disks. Asterisks indicate water impurity bands.

of the final spectrum obtained after 20 h of heating remain relatively unchanged compared to the spectrum of the sample after 5 h of heating. These observations and the fact that the sample after 5 h of heating is a brown-orange liquid point to a rather fast oxidation of V(IV) to V(V) involving the liberation of SO_2 and a slower liberation of SO_3. The endothermic two-peak feature of the DTA curve for $K_4(VO)_3(SO_4)_5$ (Fig. 6) can also be interpreted in accordance with the above two-step process. A reaction that may account for these observations and which leads to a weight loss of 21% in good agreement with the experimental data of Fig. 7 is

$$2K_4(VO)_3(SO_4)_5 \rightarrow 4KVO_2SO_4 \cdot K_2SO_4 \cdot 2KVO_3 + 3SO_2(g) + 2SO_3(g). \quad (5)$$

Figure 10 shows the spectrum of $KV(SO_4)_2$ after 13 h of heating at 490°C and also includes, for comparison, the spectrum of $K_4(VO)_3(SO_4)_5$ after 20 h of heating. The features of these two spectra are almost identical and therefore it seems that the products formed by heating and reoxidation of the two different compounds are similar. A possible reaction accounting for this and for the weight loss found experimentally by heating the sample in air is

$$2KV(SO_4)_2 + O_2(g) \rightarrow KVO_2SO_4 \cdot KVO_3 + 2SO_3(g). \quad (6)$$

Thus the reformation of melts with vanadium in the 5+ oxidation state can be achieved by heating. Furthermore, an uptake of SO_3 by the products of Eqs. (5) and (6) may take place when SO_3 is produced during the catalytic process. In this way transformation to pyrosulfate-containing

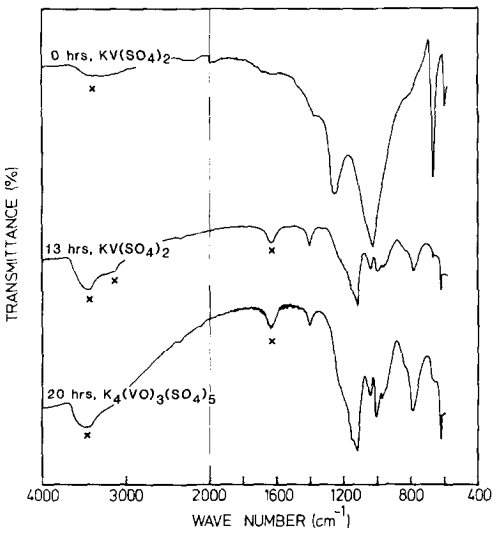

FIG. 10. Infrared spectra of the compound $KV(SO_4)_2$ before and after heating in air for 13 h. For comparison the spectrum of $K_4(VO)_3(SO_4)_5$ after heating at 490°C for 20 h in nitrogen is also shown. The spectra were taken from powdered samples pressed in KBr disks. Asterisks indicate water impurity bands.

melts will most probably occur and thereby the catalytic activity can be fully regained.

CONCLUSIONS

For the first time, crystalline compounds of V(IV) and V(III) have been isolated from V_2O_5–$M_2S_2O_7$ (M = Na, K, Cs) melts during SO_2 oxidation at temperatures in the range 350–480°C. The isolation of the compounds was performed under conditions of industrial operation using a feed gas of 10% SO_2, 11% O_2, and 79% N_2. The compounds that were isolated had the formulae $Na_2VO(SO_4)_2$, $NaV(SO_4)_2$, $K_4(VO)_3(SO_4)_5$, $KV(SO_4)_2$, $Cs_2(VO)_2(SO_4)_3$, and $CsV(SO_4)_2$.

The break in the Arrhenius-type plots for the V_2O_5–$K_2S_2O_7$ and the V_2O_5–$Cs_2S_2O_7$ molten-salt systems during SO_2 oxidation at low conversions occurs at the temperature where the low-valence vanadium compounds start precipitating. Below this temperature the apparent energy of activation for the oxidation of SO_2 increases drastically. For the V_2O_5–$Na_2S_2O_7$ melts, the phase transformation occurs already at temperatures above the measured range and the apparent activation energies are high for the whole temperature range studied (350–450°C).

The V(III) crystalline compounds preferably precipitate from melts with high M/V ratios (e.g., M/V = 10), while the V(IV) compounds predominate in precipitate from melts with low M/V ratios (e.g., M/V = 3 and 4.7).

The break in the Arrhenius-type plots occurs at lower temperatures as (i) the atomic number of the alkali promoter increases, (ii) more of the promoters are mixed, (iii) the alkali-to-vanadium ratio is increased, and (iv) the SO_3/SO_2 ratio increases.

The restoration of the catalytic activity of the melts is connected to the dissolution of the catalytically inactive crystalline compounds and is achieved by a heat treatment at temperatures above 460°C. At these temperatures, the low-valence vanadium compounds seem to decompose and reoxidize.

ACKNOWLEDGMENTS

This investigation has been supported by the General Secretariat of Research and Technology of the Greek Ministry of Industry, Energy, and Technology. Haldor Topsøe A/S is acknowledged for providing us with a sample of the catalyst VK 38. S. Boghosian is indebted to the Calouste Gulbenkian Foundation, Portugal, for a grant during the course of the present investigation. Partial support from the Danish Technical Science Research Foundation is also acknowledged.

REFERENCES

1. Villadsen, J., and Livbjerg, H., *Catal. Rev. Sci. Eng.* **17,** 203 (1978).
2. Kenney, C. N., *Catalysis (London)* **3,** 123 (1980).
3. Urbanek, A., and Trella, M., *Catal. Rev. Sci. Eng.* **21,** 73 (1980).
4. Mars, P., and Maessen, J. G. H., *in* "Proceedings, 3rd International Congress on Catalysis, Amsterdam, 1964," Vol. 1, p. 266. Wiley, New York, 1965; *J. Catal.* **10,** 1 (1968).
5. Boreskov, G. K., Polyakova, G. M., Ivanov, A. A., and Mastikhin, V. M., *Dokl. Akad. Nauk. SSSR* **210,** 626 (1973).
6. Boreskov, G. K., Davydova, L. P., Mastikhin, V. M., and Polyakova, G. M., *Dokl. Akad. Nauk. SSSR* **171,** 648 (1966); Engl. trans., p. 760.
7. Grydgaard, P., Jensen-Holm, H., Livbjerg, H., and Villadsen, J., *ACS Symp. Ser.* **65,** 582 (1978).
8. Doering, F., and Berkel, D., *J. Catal.* **103,** 126 (1987).
9. Mastikhin, V. M., Polyakova, G. M., Zyulkovskii, Y., and Boreskov, G. K., *Kinet. Katal.* **12,** 666 (1971).
10. Doering, F. J., Yuen, H. K., Berger, P. A., and Unland, M. L., *J. Catal.* **104,** 186 (1987).
11. Tandy, G. H., *J. Appl. Chem.* **6,** 68 (1956).
12. Topsøe, H. F. A., and Nielsen, A., *Trans. Dan. Acad. Tech. Sci.* **1,** 18 (1947).
13. Jensen-Holm, H., Ph.D. thesis, Technical University of Denmark, Lyngby, 1978.
14. Fehrmann, R., Hansen, N. H., and Bjerrum, N. J., *Inorg. Chem.* **22,** 4009 (1983).
15. Hansen, N. H., Fehrmann, R., and Bjerrum, N. J., *Inorg. Chem.* **21,** 744 (1982).
16. Hatem, G., Fehrmann, R., Bjerrum, N. J., and Gaune-Escard, M., in preparation.
17. Fehrmann, R., Gaune-Escard, M., and Bjerrum, N. J., *Inorg. Chem.* **25,** 1132 (1986).
18. Hatem, G., Fehrmann, R., Gaune-Escard, M., and Bjerrum, N. J., *J. Phys. Chem.* **91,** 195 (1987).
19. Bazarova, Z. G., Boreskov, G. K., Ivanov, A. A., Karakchiev, L. G., and Kochkina, L. D., *Kinet. Katal.* **12,** 948 (1971); Engl. trans., p. 845.
20. Boghosian, S., Ph.D. thesis, University of Patras, 1988.

21. (*a*) Fehrmann, R., Boghosian, S., Papatheodorou, G. N., Nielsen, K., Berg, R. W., and Bjerrum, N. J., *Inorg. Chem.* **28,** 1897 (1989); (*b*) in preparation.
22. Fehrmann, R., Krebs, B., Papatheodorou, G. N., Berg, R. W., and Bjerrum, N. J., *Inorg. Chem.* **25,** 1571 (1986).
23. Mastikhin, V. M., Lapina, O. B., Balzhinimaev, B. S., Simonova, L. G., Karnatovskaya, L. M., and Ivanov, A. A., *J. Catal.* **103,** 160 (1987).
24. Boghosian, S., Fehrmann, R., Bjerrum, N. J., and Papatheodorou, G. N., in preparation.
25. Fehrmann, R., Berg, R. W., and Bjerrum, N. J., in preparation.
26. Spitsyn, V. I., and Mikhailenko, I. E., *J. Inorg. Chem. (USSR)* **II,** 2416 (1957).
27. Flood, H., and Førland, T., *Acta Chem. Scand.* **1,** 781 (1947).
28. Simecek, A., *J. Catal.* **18,** 83 (1970).
29. Xie, K. C., and Nobile, A. J., *J. Catal.* **94,** 323 (1985).
30. Livbjerg, H., and Villadsen, J., *Chem. Eng. Sci.* **27,** 21 (1972).
31. Boreskov, G. K., and Shogam, S. M., *Zh. Fiz. Khim.* **14,** 1337 (1940).